Int. J. Electrochem. Sci., 15 **(2020)** 8311 – 8320, doi: 10.20964/2020.08.21

International Journal of
ELECTROCHEMICAL
SCIENCE
www.electrochemsci.org

Short Communication

A high-capacity catechol-based cathode material for rechargeable lithium-ion batteries

Ruiqiang Zhang[1], *Ying Zhang*[1], *Xizhong Yin*[1], *Zhiying Meng*[2], *Ya Du*[2,*] *and Haishen Yang*[1,*]

[1] Shanghai Key Laboratory of Materials Protection and Advanced Materials in Electric Power, Shanghai University of Electric Power, Shanghai 200090, China.
[2] Institute of Advanced Synthesis, School of Chemistry and Molecular Engineering, Nanjing Tech University, Nanjing 211816, China.
*E-mail: yanghsh@shiep.edu.cn, ydu@njtech.edu.cn

Received: 2 April 2020 / *Accepted:* 18 May 2020 / *Published:* 10 July 2020

Using facile acetylene trimerization as a key step, six catechols were congregated on one benzene core to develop a star-shaped redox-active molecule, namely, 3',4',5',6'-tetrakis(3,4-dihydroxyphenyl)-[1,1':2',1"-terphenyl]-3,3",4,4"-tetraol, which was termed Cat_6B. Cat_6B demonstrated as a promising cathode material for lithium ion battery with extreme low solubiliy, good cycling stability, and high theoretical specific capacity (442 mAh/g). An initial discharge specific capacity up to 305.2 mAh/g@50 mA/g and an energy density of 671 Wh/kg were achieved.

Keywords: organic cathode; catechol; lithium-ion batteries; acetylene trimerization

1. INTRODUCTION

Due to the increasing demand for inorganic electrode materials to be used in electrochemical energy storage devices (e.g., lithium-ion batteries), an energy-ecology dilemma exists, and there is a critical need for alternatives to traditional energy storage materials, especially cathode materials (e.g., $LiFePO_4$ and $LiCoO_2$); in particular, there is a need for alternatives with high energy density and sustainability [1]. Compared with inorganic cathode materials, organic cathode materials are eco-friendly and sustainable [2, 3]. Except for those readily from fossil industries, redox-active organic materials can even be derived from renewable biomass [4]. Due to the highly developed chemical technologies, redox-active organic materials can be precisely designed and manufactured under mild conditions with densely located multiple-electron-storage redox-active sites and thus with high theoretical specific capacities [5, 6]. However, one of the main problems for organic electrode materials is their dissolvability in non-aqueous electrolytes, leading to the rapid decay of energy capacity and the poor cycle stability of batteries [4, 7-10]. Various strategies have been developed to address this issue, such as the integration of redox-active moieties into various insoluble polymers. [11-13].

Oligomerizing the redox-active moieties into insoluble large molecules of certain shapes, usually with rigid backbones [14], is an efficient way to inhibit the solubility and promote the performance of organic cathode materials [15, 16]. Due to its synthetic feasibility and efficient manipulability of molecular properties, oligomerization demonstrates great potential for the development of novel organic cathode materials. However, there are only a few reports on such materials [17-19]. Moreover, the limited theoretical specific capacities of the reported oligomers need to be further improved because of the high content of redox-inactive segments in their structures [20, 21]. In particular, more-efficient synthetic strategies/approaches to construct robust redox-active large molecules are also highly desired.

Herein, a star-shaped redox-active molecule, namely, 3',4',5',6'-tetrakis(3,4-dihydroxyphenyl)-[1,1':2',1''-terphenyl]-3,3'',4,4''-tetraol, which was termed Cat$_6$B, was developed with a cobalt-catalysed acetylene trimerization reaction as the key step. Cat$_6$B is an insoluble powder solid. Cat$_6$B features six catechols on one benzene core (Scheme 1). *Ortho*-hydroquinone (e.g., catechol) could be readily oxidized and yielded *ortho*-quinone, both of which are known to have high potentials and fast electrochemical kinetics [22]. Catechol is an important chemical in pharmaceutical and material industries, mainly produced by hydroxylation of phenol or obtained from a variety of natural plants and organisms [23-25]. However, the prototype catechol cannot be directly used as electrode materials for energy storage because of its high solubility in organic electrolytes and the instability of redox radical intermediates. Through this rational molecular design, the solubility of Cat$_6$B and its redox intermediates could be greatly decreased, and thus, the stability of the redox radical intermediates could be increased [16]. Additionally, the stability of the active radical intermediates of Cat$_6$B could be increased through the enhanced inter-/intramolecular steric hindrance effects of its crowded architecture. Moreover, the electrochemical properties of Cat$_6$B might also be improved by the synergistic effects of the adjacent catechol groups. As indicated in Scheme 1, Cat$_6$B can store up to 12 electrons in one molecule and retains a high theoretical specific capacity of 442 mAh/g, which is 2.6 times that of $LiFePO_4$. Under the optimized conditions so far, an initial discharge specific capacity that has been achieved to date is 305.2 mAh/g@50 mA/g. The median discharge voltage is approximately 2.2 V. Though only 69% of its theoretical capacity is achieved, the experimental energy density is as high as 671 Wh/kg.

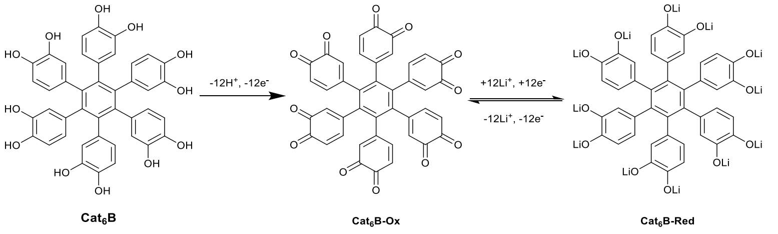

Scheme 1 Redox mechanism of Cat$_6$B.

2. EXPERIMENTAL

All commercial grade reagents and anhydrous solvents were purchased from Shanghai Titan Scientific Co., Ltd. As shown in Scheme 2, Cat$_6$B was synthesized in two steps from known 1,2-bis(3,4-dimethoxyphenyl)ethyne (1) [26] with acetylene trimerization as the key step.

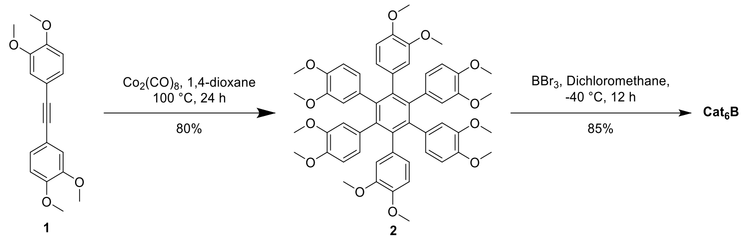

Scheme 2. Synthetic route to Cat_6B

3',4',5',6'-Tetrakis(3,4-dimethoxyphenyl)-3,3'',4,4''-tetramethoxy-1,1':2',1''-terphenyl (2) [27]: 1,2-Bis(3,4-dimethoxyphenyl)ethyne (1) (500 mg, 1.7 mmol) in anhydrous dioxane (20 mL) and $Co_2(CO)_8$ (115 mg, 0.3 mmol) were added to a 50-mL Schlenk flask under a nitrogen atmosphere, and they were stirred for 24 h at 100 °C. Then, the solvent was removed under reduced pressure. The resulting dark solid was purified by column chromatography (hexane/ethyl acetate = 5 : 1) to yield 2 (0.4 g, 80%) as a yellow solid. ^1H NMR (400 MHz, $CDCl_3$) δ = 6.45 – 6.29 (m, 18H), 3.74 -3.71 (m, 18H), and 3.44 - 3.41 (m, 18H). ^{13}C NMR (101 MHz, $CDCl_3$) δ = 147.98, 147.02, 140.69, 134.01, 124.47, 115.88, 110.23, and 56.09. HRMS (ESI): *m/z* $[M+H]^+$ calcd for $[C_{54}H_{55}O_{12}]^+$ 895.3694, found 895.3696.

3',4',5',6'-Tetrakis(3,4-dihydroxyphenyl)-[1,1':2',1''-terphenyl]-3,3'',4,4''-tetraol (Cat_6B) [28]: BBr_3 (1.3 g, 5 mmol) was slowly dropped to a suspension of compound 2 (300 mg, 0.3 mmol) in dry dichloromethane (15 mL) in a 50-mL Schlenk flask at -80 °C under a nitrogen atmosphere. Then, the temperature of the reaction mixture was gradually allowed to reach room temperature and stirred for 12 h. A 2 M NaOH solution (20 mL) was poured into the reaction mixture. Then, the aqueous layer was washed with dichloromethane, acidified with a 3 M HCl solution (20 mL), extracted with ethyl acetate (25 mL × 3) and backwashed with water (25 mL). The organic phase was dried over anhydrous sodium sulfate and then concentrated under reduced pressure. The crude product was purified by column chromatography (methanol/hexane = 3 : 1) to yield Cat_6B (0.9 g, 85%) as a blue black powder solid. ^1H NMR (400 MHz, CD_3OD) δ = 6.33 - 6.26 (m, 12H), and 6.19 (s, 6H). ^{13}C NMR (126 MHz, CD_3OD) δ = 149.13, 146.37, 134.54, 125.91, 125.21, and 100.31. HRMS (ESI): *m/z* $[M+H]^+$ calcd for $[C_{42}H_{31}O_{12}]^+$ 727.1816, found 727.1816.

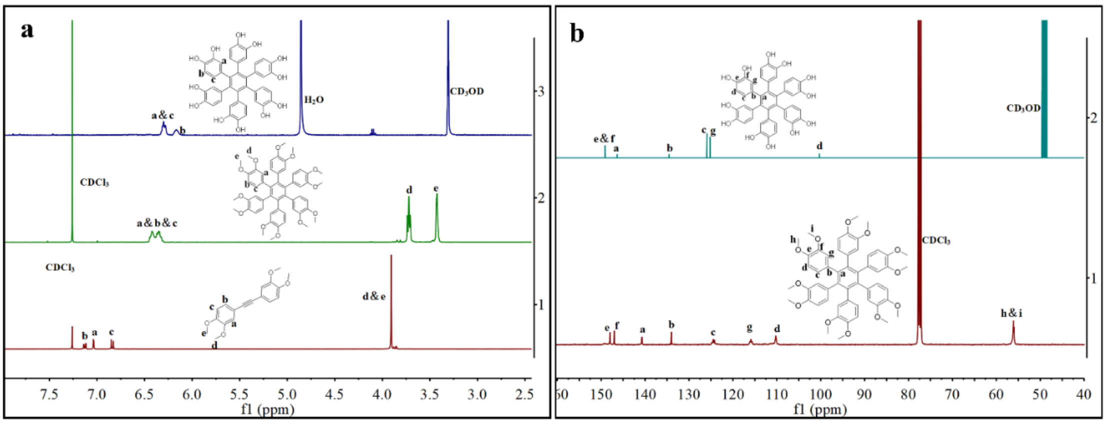

Figure 1. a) ^1H NMR spectroscopy, b) ^{13}C NMR spectroscopy.

Organic electrodes were fabricated using the following steps. The active material, conductive agent, and polyvinylidene fluoride (PVDF, 2.5 wt% in NMP) binder of all batteries were mixed in a ratio of 5 : 4 : 1. The mixture was stirred with a mechanical stirrer for 2 h at room temperature and coated onto an aluminium foil substrate with a blade set to a thickness of 200 µm. Coatings were dried in a vacuum oven at 80 °C for 12 h and then cut into circular electrode discs with diameters of 14 mm. After the electrode discs were weighed, they were transferred into a glove box and assembled under an argon atmosphere into lithium-ion batteries using CR2016 coin-type cell hardware, with lithium foil as the counter electrode and polypropylene as the separator. The galvanostatic discharge/charge tests in the voltage range of 1.2–4.0 V at different current densities were carried out on a CT-4008-5 V 10 mA-164 Battery Tester (Shenzhen Neware Technology Limited Company). Cyclic voltammograms (CVs) were carried out (voltage: 1.2–4.0 V, scan rate: 1 mV/s) by a CS350H electrochemical workstation (Wuhan Corrtest Instruments Corp., Ltd.)

3. RESULTS AND DISCUSSION

With Cat_6B in hand, we first optimized the electrolytes. Two typical electrolyte systems were studied, i.e., 1 M LiTFSI-DOL/DME (DOL: 1,3-dioxolane, DME: 1,2-dimethoxyethane) and 1 M $LiPF_6$-EC/DMC/DEC (EC: ethylene carbonate, DMC: dimethyl carbonate, and DEC: diethyl carbonate), with carbon black as the conductive additive. At a current density of 50 mA/g, the cycle performance comparison curve shows that the initial discharge specific capacity in the carbonate-based electrolyte was 111 mAh/g, and the capacity retention rate was 52.3% after 100 cycles. In the ether-based electrolyte, the initial discharge specific capacity was 90 mA/g, and the capacity retention ratio was 85.3% at the same current density (Figure 2). Cat_6B had better cycle stability in ether-based electrolytes. There are two possible reasons for this result.

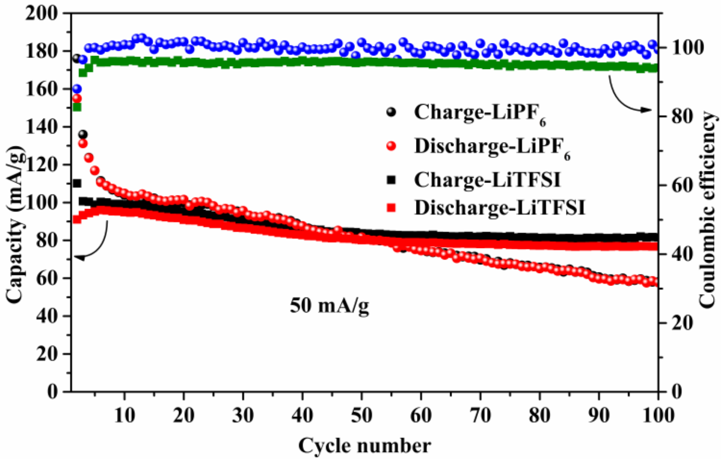

Figure 2. Cycle performance of Cat_6B with different electrolytes (carbon black).

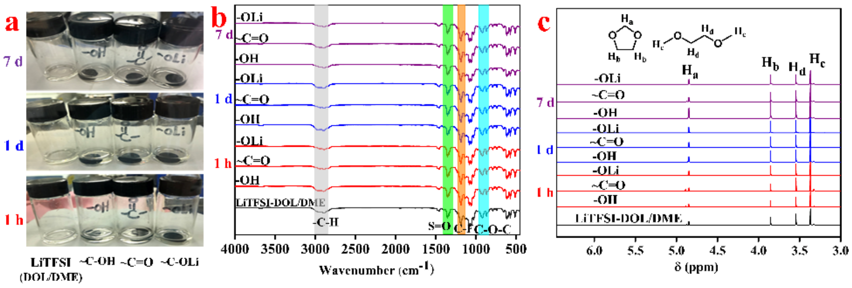

Figure 3. a) Photographs of the pristine electrolyte (1 M LiTFSI-DOL/DME) and Cat_6B, Cat_6B-Ox, and Cat_6B-Red electrodes soaked in the electrolyte for different time intervals, b) FTIR spectroscopy of the pristine electrolyte, and the electrolytes with Cat_6B, Cat_6B-Ox and Cat_6B-Red soaked for different time intervals, c) ^1H NMR spectroscopy of the pristine electrolyte, and the electrolytes with Cat_6B, Cat_6B-Ox and Cat_6B-Red soaked in for different time intervals.

First, Cat_6B and its redox reaction species are more soluble in high-polar carbonate-based electrolytes than in a low-polar ether-based electrolyte. The active species could gradually dissolve in the organic electrolytes during the charge-discharge process, resulting in a decrease in the specific capacity of Cat_6B. Another possible reason is that the catecholate anions generated during the electrochemical process would undergo transesterification slowly with the carbonate esters and capture the reduced oxygen anions. The redox reaction is then terminated; thus, the cycle performance and capacity retention decrease gradually over time.

To confirm the solubility of the redox species of Cat_6B in the electrolyte, we further studied the solubility of Cat_6B (~C-OH), together with its typical redox intermediates during the charge-discharge process (Scheme 1), i.e., quinone (~C=O, Cat_6B-Ox) and lithium catecholate (~C-OLi, Cat_6B-Red) in an electrolyte (1 M LiTFSI-DOL/DME). Cat_6B-Ox was obtained from Cat_6B through a full charge in the battery. Cat_6B-Red was obtained from Cat_6B through a charge and discharge cycle in the battery. The dissolution of Cat_6B, Cat_6B-Ox and Cat_6B-Red in the electrolytes was tested by examining the electrolytes after the electrodes with the corresponding species were soaked in for different time intervals. As the soaking time increased from 1 hour to 7 days, no noticeable colour change was observed (Figure 3a), indicating that those species have no obvious solubility in the electrolytes. To further confirm the insolubility of Cat_6B, Cat_6B-Ox and Cat_6B-Red, we performed ^1H NMR spectroscopy and FTIR spectroscopy on the electrolytes (Figure 3b and 3c). The FTIR spectroscopy showed no characteristic peaks from Cat_6B species except for the solute $LiN(CF_3SO_2)_2$ peaks and solvent (DOL/DME) peaks of the electrolyte. The ^1H NMR spectroscopy only demonstrated the characteristic resonances for DOL and DME at 4.85, 3.85, 3.54, and 3.36 ppm (Figure 3c, 3.31 ppm CD_3OD, 4.87 ppm water). There were no observable signals corresponding to Cat_6B, Cat_6B-Ox or Cat_6B-Red in the nine samples, further indicating that redox-active species do not obviously dissolve in the 1 M LiTFSI-DOL/DME. The above experimental results support that ether electrolyte (1 M LiTFSI-DOL/DME) is a suitable electrolyte system for Cat_6B.

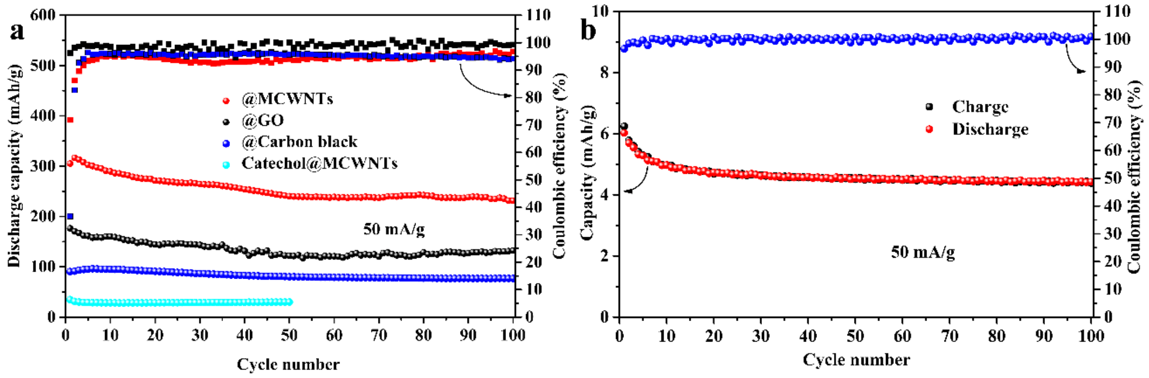

Figure 4. a) Cycle performance of different cathode materials (Cat_6B and Catechol) with different conductive agents (1 M LiTFSI-DOL/DME), b) Cycle performance of MCWNTs (MCWNTs/PVDF=4/6, 1 M LiTFSI-DOL/DME).

Next, different conductive additives were screened to optimize the performance, including multiwalled carbon nanotubes (MCWNTs), graphene oxide (GO) and carbon black. The cathode composite of Cat_6B, conductive additive, and binder (polyvinylidene fluoride, PVDF) were employed at a ratio of 5 : 4 : 1. As indicated in Figure. 4a, when MCWNTs were used as the conductive additive, the initial discharge specific capacity reached 305.2 mAh/g, and Cat_6B maintained a high discharge specific capacity of 231.4 mAh/g after 100 cycles. When carbon black and GO were used instead, the discharge specific capacities were 76.8 mAh/g and 132.2 mAh/g, respectively, after the same cycling numbers. MCWNTs is the best conductive agent for Cat_6B. This might be due to the different morphologies of the other conductive additives. Compared with granular carbon black and sheet-lamellar GO, MCWNTs has a one-dimensional tubular structure and very high specific surface area, which makes it easier to form an effective, high-strength conductive network. The cross-linked conductive network formed in the electrode can effectively improve the electrochemical performance of Cat_6B [29, 30]. We also measured the capacity contribution of the MCWNTs, which was approximately 5 mAh/g (Figure 4b).

Table 1. A comparison with relevant literature reports.

Active material	Electrolyte	Initial discharge capacity (mAh/g)	Cycling stability: retention, cycles, current	Ref
(−)-NDI-Δ	1 M LiTFSI in DOL : DME with 0.2 M $LiNO_3$(1 : 1 v/v)	146.4 (0.1 C)	71.1%, 300, 10 C	[31]
(−)-3PMDI-Δ	$LiPF_6$ in EC : DMC (1 : 1 v/v)	134.75 (0.2 C)	64%, 50, 0.2 C	[32]
TPB	1 M LiTFSI in DOL : DME (1 : 1 v/v)	223.2 (0.1 C)	91.4%, 100, 0.2 C	[20]
LCPYT	1 M $LiPF_6$ in PC	217 (0.2 C)	78%, 100, 0.2 C	[33]
3Q	1 M $LiClO_4$ in EC/DEC (1 : 1 v/v)	250 (0.2 C)	80%, 30, 0.2 C	[34]
NDA-4N	1 M LiTFSI in DOL : DME with 1% $LiNO_3$(1 : 1 v/v)	141.8 (66 mA/g)	34.4%, 99, 66 mA/g	[35]
PDA-4N	1 M LiTFSI in DOL : DME	116.3	70.9%, 99, 66 mA/g	[35]

	with 1% $LiNO_3$(1 : 1 v/v)	(66 mA/g)		
C_6O_6	0.3 M LiTFSI-[PY13]-[TFSI]	902 (20 mA/g)	82%, 100, 50 mA/g	[15]
P5Q	PMA/PEG-$LiClO_4$-3 wt% SiO_2	418 (0.2 C)	94.7%, 50, 0.2 C	[36]
Cat_6B	1 M LiTFSI in DOL : DME (1 : 1 v/v)	305.2 (50 mA/g)	75.8%, 100, 50 mA/g	This work

(−)-NDI-Δ = triangular shaped naphthalenediimide, (−)-3PMDI-Δ = cyclic trimeric pyromellitic diimide, TPB = 2,3,5,6-tetraphthalimido-1,4-benzoquinon, LCPYT = 2,7-bis(lithiooxycarbonyl)pyrene-4,5,9,10-tetraone, 3Q = Hexaazatrinaphthylene, NDA-4N = 1,4,5,8-naphthalenetetracarboxylic, PDA-4N = 3,4,9,10-perylenetetracarboxylic dianhydrid, C_6O_6 = Cyclohexanehexone, P5Q = Pillar[5]quinone.

Table 1 depicts the electrochemical performance of organic small molecule electrode materials reported in other articles, in which the active material, electrolyte, initial discharge specific capacity, current density, cycle number and capacity retention content are listed. Through this comparison, we can find that Cat_6B has a relatively high initial discharge specific capacity; moreover, after 100 cycles at a current density of 50 mA/g, its capacity retention rate was 75.8%, and it maintained a high capacity retention. This finding also shows that Cat_6B had excellent electrochemical performance.

Next, the rate performance of Cat_6B was investigated under the optimized conditions (MCWNTs, 1 M LiTFSI-DOL/DME). The Cat_6B-based battery showed stable reversible capacities of 240, 221, 204, and 176 at current densities of 50, 100, 200 and 500 mA/g (Figure 5a), respectively. Even at a current density of 500 mA/g, the capacity of Cat_6B was 176 mAh/g, which is equivalent to 58% of the initial capacity. We used cyclic voltammetry (CV) to measure the redox activity of Cat_6B in lithium batteries. Figure 5b shows that Cat_6B has a broad redox peak, which is also a typical characteristic peak of the catechol redox centre [37, 38]. The charge-discharge curves of Cat_6B were sloping (Figure 5c), which can be attributed to the multielectron continuous redox process of Cat_6B [15]. This phenomenon was also reported in inorganic electrode materials [39]. As a comparison, a cell with the parent catechol as the cathode material was also tested under otherwise identical conditions (Figure 4a). Only 6% of its theoretical capacity was observed. This experimental capacity is only 12% of the capacity of Cat_6B. This result clearly demonstrates the remarkable effectiveness of this oligomerization strategy. The stable cycling performance of catechol is attributed to the formation of polymers from its unstable electro-oxidation products, *ortho*-quinone and radical species [40].

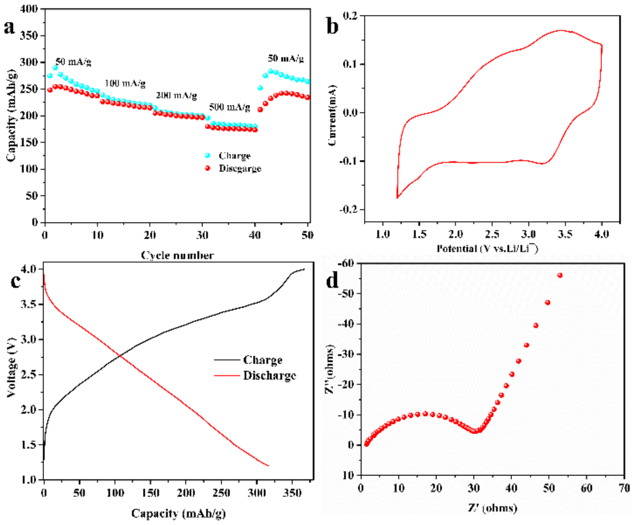

Figure 5. a) Rate performance of Cat_6B at different current densities (MCWNTs, 1 M LiTFSI-DOL/DME), b) Cyclic voltammetry (CV) measurement of Cat_6B (MCWNTs, 1 M LiTFSI-DOL/DME), c) Charge-discharge curves of Cat_6B (MCWNTs, 1 M LiTFSI-DOL/DME), d) Electrochemical impedance spectroscopy of Cat_6B (MCWNTs, 1 M LiTFSI-DOL/DME).

4. CONCLUSIONS

In summary, we successfully designed and synthesized a star-shaped catechol-rich molecule, namely, Cat_6B, through a facile oligomerization approach. Cat_6B can store up to 12 electrons and has a theoretical specific capacity of 442 mAh/g. This capacity is among the highest of well-studied organic cathode materials and greatly surpasses all the known transition-metal-based cathode materials. Catechol-united Cat_6B has a cramped construction and a low solubility in organic electrolytes, which efficiently promote the stability of normally unstable organic redox intermediates. When used as cathode materials for lithium-ion batteries, Cat_6B demonstrated good cycling stability. The experimental specific capacity of Cat_6B was greatly improved compared with its parent catechol. This work provides an efficient and feasible strategy to develop high-capacity organic cathode materials and demonstrates the remarkable potential of redox-active organic molecules as sustainable and eco-friendly cathode materials with high energy densities for practical applications.

ACKNOWLEDGEMENTS
H. Y. thanks the financial supports from Science and Technology Commission of Shanghai Municipality (19DZ2271100), and Program for Professor of Special Appointment (Eastern Scholar) at Shanghai Institutions of Higher Learning. Y. D. thanks National Natural Science Foundation of China (21805134), Natural Science Foundation of Jiangsu Province, China (BK20191363), Science and Technology Innovation Project for Overseas Students from Nanjing City, and Start-up Grant Nos. 39837141 from NJTECH. The authors thank Prof. Honghua Ge’s group for the assistance of FTIR measurements.

References

1. N.S. Lewis, *Science*, 351 (2016) aad1920.

2. Z. Zhao-Karger, P. Gao, T. Ebert, S. Klyatskaya, Z. Chen, M. Ruben, M. Fichtner, *Adv. Mater.*, 31 (2019) 1806599.
3. P. Poizot, F. Dolhem, *Energy Environ. Sci.*, 4 (2011) 2003.
4. N. Patil, A. Aqil, F. Ouhib, S. Admassie, O. Inganäs, C. Jérôme, C. Detrembleur, *Adv. Mater.*, 29 (2017) 1703373.
5. E.J. Son, J.H. Kim, K. Kim, B.P. Chan, *J. Mater. Chem. A*, 4 (2016) 11179.
6. S. Lee, G. Kwon, K. Ku, K. Yoon, S.-K. Jung, H.-D. Lim, K. Kang, *Adv. Mater.*, 30 (2018) 1704682.
7. Z.Q. Zhu, J. Chen, *J. Electrochem. Soc.*, 162 (2015) A2393.
8. Q. Zou, W. Wang, A. Wang, Z. Yu, K. Yuan, *Mater. Lett.*, 117 (2014) 290.
9. D. Wu, H. Li, R. Li, Y. Hu, X. Hu, *Chem. Commun.*, 54 (2018) 11415.
10. H.-g. Wang, S. Yuan, Z. Si, X.-b. Zhang, *Energy Environ. Sci.*, 8 (2015) 3160.
11. S. Wang, Q. Wang, P. Shao, Y. Han, X. Gao, L. Ma, S. Yuan, X. Ma, J. Zhou, X. Feng, B. Wang, *J. Am. Chem. Soc.*, 139 (2017) 4258.
12. S. Gu, S. Wu, L. Cao, M. Li, N. Qin, J. Zhu, Z. Wang, Y. Li, Z. Li, J. Chen, Z. Lu, *J. Am. Chem. Soc.*, 141 (2019) 9623.
13. J. Wang, Y. Lee, K. Tee, S.N. Riduan, Y. Zhang, *Chem. Commun.*, 54 (2018) 7681.
14. S.K.M. Nalluri, Z. Liu, Y. Wu, K.R. Hermann, A. Samanta, D.J. Kim, M.D. Krzyaniak, M.R. Wasielewski, J.F. Stoddart, *J. Am. Chem. Soc.*, 138 (2016) 5968.
15. Y. Lu, X. Hou, L. Miao, L. Li, R. Shi, L. Liu, J. Chen, *Angew. Chem. Int. Ed.*, 58 (2019) 7020.
16. S. Wu, W. Wang, M. Li, L. Cao, F. Lyu, M. Yang, Z. Wang, Y. Shi, B. Nan, S. Yu, Z. Sun, Y. Liu, Z. Lu, *Nat. Commun.*, 7 (2016) 13318.
17. J. Wang, K. Tee, Y. Lee, S.N. Riduan, Y. Zhang, *J. Mater. Chem. A*, 6 (2018) 2752.
18. D.J. Kim, D.-J. Yoo, M.T. Otley, A. Prokofjevs, C. Pezzato, M. Owczarek, S.J. Lee, J.W. Choi, J.F. Stoddart, *Nat. Energy*, 4 (2019) 51.
19. C. Peng, G.-H. Ning, J. Su, G. Zhong, W. Tang, B. Tian, C. Su, D. Yu, L. Zu, J. Yang, M.-F. Ng, Y.-S. Hu, Y. Yang, M. Armand, K.P. Loh, *Nat. Energy*, 2 (2017) 17074.
20. Z. Luo, L. Liu, Q. Zhao, F. Li, J. Chen, *Angew. Chem. Int. Ed.*, 56 (2017) 12561.
21. S. Oda, T. Shimizu, T. Katayama, H. Yoshikawa, T. Hatakeyama, *Org. Lett.*, 21 (2019) 1770.
22. Y. Lu, Q. Zhang, L. Li, Z.Q. Niu, J. Chen, *Chem*, 4 (2018) 2786.
23. M. Krogsgaard, V. Nue, H. Birkedal, *Chem. Eur. J.*, 22 (2016) 844.
24. C. Huang, N. Ghavtadze, B. Chattopadhyay, V. Gevorgyan, *J. Am. Chem. Soc.*, 133 (2011) 17630.
25. C. Rice-Evans, N. Miller, G. Paganga, *Trends Plant Sci.*, 2 (1997) 152.
26. L. Li, C. Ni, F. Wang, J. Hu, *Nat. Commun.*, 7 (2016) 13320.
27. Z. Wang, F. Dötz, V. Enkelmann, K. Müllen, *Angew. Chem. Int. Ed.*, 44 (2005) 1247.
28. K. Kobayashi, T. Shirasaka, A. Sato, E. Horn, N. Furukawa, *Angew. Chem. Int. Ed.*, 38 (1999) 3483.
29. Q.T. Zhang, Z.L. Yu, P. Du, C. Su, *Recent Pat. Nanotechnol.*, 4 (2010) 100.
30. X. Li, F. Kang, W. Shen, *Electrochem. Solid-State Lett.*, 9 (2006) A126.
31. D. Chen, A.-J. Avestro, Z. Chen, J. Sun, S. Wang, M. Xiao, Z. Erno, M.M. Algaradah, M.S. Nassar, K. Amine, Y. Meng, J.F. Stoddart, *Adv. Mater.*, 27 (2015) 2907.
32. D.J. Kim, K.R. Hermann, A. Prokofjevs, M.T. Otley, C. Pezzato, M. Owczarek, J.F. Stoddart, *J. Am. Chem. Soc.*, 139 (2017) 6635.
33. A. Shimizu, H. Kuramoto, Y. Tsujii, T. Nokami, Y. Inatomi, N. Hojo, H. Suzuki, J.-i. Yoshida, *J. Power Sources*, 260 (2014) 211.
34. Y. Hanyu, T. Sugimoto, Y. Ganbe, A. Masuda, I. Honma, *J. Electrochem. Soc.*, 161 (2013) A6.
35. J. Xie, W. Chen, Z. Wang, K.C.W. Jie, M. Liu, Q. Zhang, *Chem. Asian J.*, 12 (2017) 868.
36. Z. Zhu, M. Hong, D. Guo, J. Shi, Z. Tao, J. Chen, *J. Am. Chem. Soc.*, 136 (2014) 16461.
37. T. Liu, K.C. Kim, B. Lee, Z. Chen, S. Noda, S.S. Jang, S.W. Lee, *Energy Environ. Sci.*, 10 (2017) 205.

38. N. Wang, D. Hou, Q. Li, P. Zhang, H. Wei, Y. Mai, *ACS Applied Energy Materials*, 2 (2019) 5816.
39. V. Augustyn, P. Simon, B. Dunn, *Energy Environ. Sci.*, 7 (2014) 1597.
40. S. Uchiyama, Y. Hasebe, T. Ishikawa, J. Nishimoto, *Anal. Chim. Acta*, 351 (1997) 259